The International Journal of Cardiovascular Imaging (2018) 34:1485–1491
https://doi.org/10.1007/s10554-018-1363-8

ORIGINAL PAPER

Patient-related factors influencing detectability of coronary arteries in 320-row CT angiography in infants with complex congenital heart disease

Yuzo Yamasaki[1] · Satoshi Kawanami[2] · Takeshi Kamitani[1] · Koji Sagiyama[1] · Seitaro Shin[1] · Takuya Hino[1] · Hazumu Nagata[3] · Hidetake Yabuuchi[4] · Michinobu Nagao[5] · Hiroshi Honda[1]

Received: 22 January 2018 / Accepted: 29 April 2018 / Published online: 5 May 2018

Abstract

To investigate the performance of second-generation 320-row computed tomographic (CT) angiography (CTA) in detecting coronary arteries and identify factors influencing visibility of the coronary arteries in infants with complex congenital heart disease (CHD). Data of 60 infants (aged 0–2 years, median 2 months) with complex CHD who underwent examination using 320-row CTA with low-dose prospective electrocardiogram-triggered volume target scanning were reviewed. The coronary arteries of each infant were assessed using a 0–4-point scoring system based on the number of coronary segments with a visible course. Clinical parameters, the CT value in the ascending aorta, image noise, and the radiation dose were subjected to univariate and multivariate analyses. The mean coronary score for all examinations was 2.6 ± 1.5 points. The mean attenuation in the ascending aorta was 306.7 ± 66.2 HU and the mean standard deviation was 21.7 ± 4.4. The mean effective radiation dose was 1.27 ± 0.39 mSv. Multivariate regression analysis showed significant correlations between coronary score and body weight ($p < 0.05$) and between coronary score and the CT value in the ascending aorta ($p < 0.02$). Second-generation 320-row CTA with prospective electrocardiogram-triggered volume target scanning and hybrid iterative reconstruction allows good visibility of the coronary arteries in infants with complex CHD. Body weight and the CT value in the ascending aorta are important factors influencing the visibility of the coronary arteries in infants.

Keywords Congenital heart defect · CT angiography · Coronary arteries · Infants · Coronary vessel anomalies

Abbreviations

CCA Conventional cardiac angiography
CHD Congenital heart disease
CT Computed tomography
ECG Electrocardiogram

✉ Yuzo Yamasaki
yyama@radiol.med.kyushu-u.ac.jp

[1] Department of Clinical Radiology, Graduate School of Medical Sciences, Kyushu University, 3-1-1 Maidashi, Higashi-ku, Fukuoka 812-8582, Japan

[2] Department of Molecular Imaging & Diagnosis, Graduate School of Medical Sciences, Kyushu University, Fukuoka, Japan

[3] Department of Pediatrics, Graduate School of Medical Sciences, Kyushu University, Fukuoka, Japan

[4] Department of Health Sciences, Graduate School of Medical Sciences, Kyushu University, Fukuoka, Japan

[5] Department of Diagnostic Imaging and Nuclear Medicine, Tokyo Women's Medical University, Fukuoka, Japan

Introduction

In patients with complex congenital heart disease (CHD), such as those with tetralogy of Fallot or transposition of the great arteries, evaluation of the anatomy of the coronary arteries is very important [1]. This is because some variations in the anatomy of the coronary arteries can contribute significantly to morbidity and mortality during surgical correction and impact management strategies [2, 3].

Recently, the spatial and temporal resolution of multislice computed tomography (CT) has been greatly improved, and this method has been increasingly used in the diagnosis of CHD in infants and young children. The image quality of cardiac CT depends heavily on the specifications of the CT machine. The faster the scan time, the better image quality can be in infants who cannot hold their breath. Scans obtained using second-generation 320-row CT prospective electrocardiogram (ECG) gating take only 0.275 s to acquire because of the faster gantry rotation and 16 cm z-axis coverage in almost all patients with complex CHD. Because the

temporal resolution of this latest CT with the volume scanning mode can reach 137.5 ms, and the volume scanning mode can achieve 180°/360° without moving, achieving all information data of all organs to avoid the migration data error caused by placement movement of patients from spiral scanning, the time interval difference of image composition, and unnecessary scan dose brought by the repetitive scanning [4]. In clinical practice, a shorter scan time is required in sedated children who cannot breath-hold. Further, this imaging mode is suitable for cardiac CT angiography (CTA) in patients with a high heart rate, especially infants and children, and may be the best method for evaluating infants with complex CHD. Further, the combination of low-tube voltage and a hybrid iterative reconstruction technique can lower the radiation exposure without impairing image quality [5, 6].

Transthoracic echocardiography is the generally preferred method for diagnosis of CHD, but the limits of the acoustic window, poor spatial resolution, and the subjectivity of the operator's judgments are major drawbacks of this procedure [7]. In addition, transthoracic echocardiography has high diagnostic ability to evaluate coronary artery patterns, especially in transposition of the great arteries; however, the assessment of coronary anomalies is sometimes difficult, and additional imaging test is required to confirm the diagnosis. Therefore, there is interest in using cardiac CTA to detect coronary anomalies in young children. However, the visibility of the coronary arteries on free-breathing cardiac CTA could be influenced by many factors, including age, body size, heart rate, radiation exposure, coronary enhancement, and the signal to noise ratio. To date, there have been no studies addressing this issue. The aim of this study was to explore the ability of free-breathing prospective ECG-triggering 320-row CTA to detect the coronary arteries in infants with complex CHD and to identify factors influencing the visibility of the coronary arteries when using this technique.

Materials and methods

The study protocol was approved by the institutional review board of our institution. The need for written informed consent was waived in view of the retrospective nature of the research. The study included 60 consecutive infants with complex CHD (37 boys and 23 girls, 0–2 years, median 2 months) who underwent examination using 320-row CTA with free-breathing prospective ECG-triggered volume target scanning between August 2015 and January 2017. Patient characteristics are shown in Table 1. CTA is performed at our institution as part of the cardiovascular evaluation in patients with complex CHD depending on clinical indications. Complex CHD is defined as CHD with more than one distinct cardiovascular anomaly, and all anomalies, including coronary anomalies, were confirmed in our patients based on surgical and/or conventional cardiac angiography (CCA) findings (Table 2).

Table 1 Patient characteristics and primary cardiovascular diagnoses in a cohort of 60 infants

Parameter	Value
Age	10 days ~1 year and 9 months
Sex (male/female)	37/23
Body weight (g)	4846 ± 2298
Heart rate (bpm)	129 ± 14
Primary cardiovascular diagnosis	
Coarctation of the aorta	12
Tetralogy of Fallot	7
Atrioventricular septal defect	6
Single ventricle	6
Ventricular septal defect	5
Patent ductus arteriosus	4
Double outlet right ventricle	4
Congenitally corrected TGA	4
Anomalous pulmonary venous return	3
Pulmonary atresia with ventricular septal defect	3
Anomalous origin of pulmonary artery	2
Interrupted aortic arch	1
Pulmonary vein stenosis	1
Transposition of great arteries (TGA)	1
Truncus arteriosus communis	1

Table 2 Diagnoses of cardiovascular deformities in a cohort of 60 infants

Cardiovascular malformations	n
Atrial septal defect/patent foramen ovale	23
Ventricular septal defect	18
Patent ductus arteriosus	18
Coarctation of the aorta	11
Single ventricle	11
Atrioventricular septal defect	8
Tetralogy of Fallot	7
Double outlet right ventricle	7
Pulmonary vein stenosis	6
Anomalous pulmonary venous return	4
Congenitally corrected TGA	4
Pulmonary atresia with ventricular septal defect	3
Anomalous origin of pulmonary artery	2
Interrupted aortic arch	1
Transposition of great arteries (TGA)	1
Truncus arteriosus communis	1
Total	125

320-row CT scan protocol

The cardiac examinations were performed using a second-generation 320-detector row CT scanner (Aquilion ONE Vision; Toshiba Medical Systems; Nasu, Japan), which has a detector width of 160 mm and 320 detector rows. The CT gantry has a minimum rotation time of 275 ms. All tests using 320-row CTA with prospective ECG-triggered mode were performed while the children were breathing freely. Intravenous thiamylal, under adequate cardiorespiratory monitoring, was used for sedation during the procedure and the dose administered was based on each child's body weight and clinical circumstances. Iodinated contrast medium (Iopamiron; 300 mg I/mL; Bayer; Osaka, Japan) was injected via a peripheral vein using a double-head power injector (Nemoto Kyorindo Co. Ltd., Tokyo, Japan) at a volume of 2.0 mL/kg body weight followed by a saline chaser of 0.67 mL/kg body weight. The injection rate was calculated as the total injected volume divided by 80 s and the data acquisition was performed at 80 s. For example, a 6-kg baby would be injected with 12 mL of contrast medium and 4 mL of saline at a flow rate of 0.2 mL/s. The scan volume was set to the whole chest, extending from the thoracic inlet superiorly to just below the diaphragm inferiorly. In patients suspected to have heterotaxy or anomalous inferior vena cava drainage, the scan volume was extended to the infrahepatic region. The patients were scanned using a prospective triggered target CTA volume scan with a rotation time of 0.275 s and a tube voltage of 80 kVp. The centre for the data acquisition phase window in this study was set to 45% of the R–R interval. The scan range, dependent on patient size, heart rate, and area to be evaluated, varied from 10 to 16 cm, and the tube current was set by automatic exposure control (noise level, standard deviation 20; thickness, 0.5 mm). The effective dose was derived from the dose-length product and conversion coefficients for the chest, taking into account the patient's age [8]. The specific dose-length product conversion coefficients for infants differed by age range: < 4 months, 0.039 mSv/[mGy cm] conversion coefficient; 4 months to 1 year of age, 0.026 mSv/[mGy cm]; 1–2 years, 0.018 mSv/[mGy cm].

Image post-processing and analysis

Full volumes were reconstructed in 0.5 mm-thickness slices. In addition to the CT axial images, multiplanar reconstruction images can also be used to display malformations of the heart and coronary vessels.

The CT images were interpreted by two board-certified radiologists (SK and KS, both with over 5 years of diagnostic experience in cardiac radiology) blinded to the results of surgery, CCA, or transthoracic echocardiography. The proximal right coronary artery running in the right atrioventricular groove, left main trunk, proximal left anterior descending artery running in the anterior interventricular sulcus, and proximal left circumflex artery running in the left atrioventricular groove were assessed in each infant and a score was allocated based on the number of coronary segments with a clearly visible course using a 0–4-point scoring system. When the left main trunk did not exist because of an anomalous origin of the left anterior descending artery or left circumflex artery, we considered the ostium of the left anterior descending artery as the left main trunk. Distal segments were not included in this evaluation because assessment of the distal coronary artery segments is not always necessary to identify coronary artery anomalies [9, 10]. The highest possible score was 4 and the lowest possible score was 0 for each patient. In the event of disagreement between the two observers, the mean of the two results was used for the coronary score.

Image quality was assessed using axial source images as follows. The mean CT attenuation in the ascending aorta was measured by placing a round region of interest (ROI). The image noise was determined as the standard deviation of the attenuation value in a single round ROI placed in the ascending aorta. The ROI was drawn as large as the diameter of the aortic lumen, while carefully avoiding the wall.

Statistical analysis

The measured data are shown as means ± standard deviations and the grouped data are expressed as percentages. Correlations between the coronary score and the other study parameters were analysed using Pearson's correlation coefficients and multivariate regression analysis. Receiver-operating characteristic curve analysis was performed to determine the optimal cutoff for the selected parameter in relation to the diagnostic imaging of all coronary arteries (irrespective of the coronary score). p Values < 0.05 were considered statistically significant. Statistical analyses were performed using JMP statistical software (version 11.0.0; SAS Institute, Cary, NC, USA).

Results

The mean coronary score for all examinations was 2.6 ± 1.5 points. The mean attenuation in the ascending aorta was 306.7 ± 66.2 HU and the mean standard deviation was 21.7 ± 4.4. The mean heart rate was 129.4 ± 13.9 bpm. The mean dose-length product was 45.71 ± 18.75 mGy cm and the mean effective radiation dose was 1.27 ± 0.39 mSv.

Univariate analysis showed moderate correlations between the coronary score and some of the study parameters (Table 3). Multivariate regression analysis showed significant correlations between coronary score and body

Table 3 Pearson correlation coefficients of coronary scores

Parameter	Pearson r	p
Body weight	0.64	< 0.001*
Heart rate	− 0.53	< 0.001
Sex	− 0.02	0.89
DLP	0.62	< 0.001*
Ao CT value	0.26	0.04*
Ao noise	− 0.023	0.86

*Statistically significant

Table 4 Multivariate linear regression model for predicting coronary scores

Parameter	Parameter estimate	Standard error	p
Intercept	1.37	2.08	
Body weight	0.00023	0.00011	0.049*
Heart rate	− 0.018	0.012	0.14
DLP	0.018	0.014	0.19
Ao CT value	0.0052	0.0021	0.017*

$R^2 = 0.530$, $F = 15.5$ ($p < 0.001$)

*Statistically significant

with an AUC of 0.92, a sensitivity of 92%, and a specificity of 83% (Fig. 1).

Eight coronary anomalies were diagnosed based on surgical findings and/or CCA (Table 5). All anomalies were detected using coronary CTA. Some examples include the following: A boy with the right coronary artery and left circumflex artery arising from the same cusp was evaluated at the age of 1 month, and 1 year and 6 months (Fig. 2). A single coronary artery is clearly depicted in a patient with a complete atrioventricular septal defect and asplenia (Fig. 3). In another patient with a single right ventricle, the CT image shows both a right coronary artery and a left circumflex artery arising separately from the non-coronary sinus of Valsalva (Fig. 4). In five patients with TOF, both CTA and echocardiography indicated that coronary anomalies were not present.

Discussion

This 320-row cardiac CT study of the detectability of coronary arteries in infants with complex CHD demonstrated that second-generation 320-row CTA with prospective

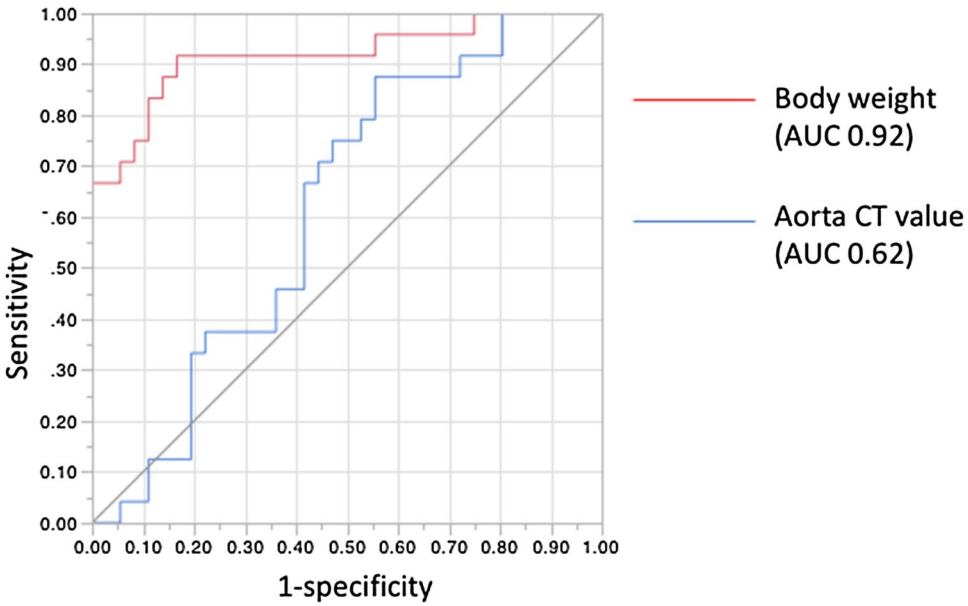

Fig. 1 Receiver-operating characteristic analysis of body weight and CT value in ascending aorta for diagnostic images of the right and left coronary arteries. The area under the receiver-operating characteristic curve of body weight is 0.92

weight and between coronary score and the CT value in the ascending aorta (Table 4).

Receiver-operating characteristic curve analysis showed that the area under curve (AUC) of body weight is higher than that of CT value in the ascending aorta. It revealed an optimal body weight threshold of 4.74 kg for identifying patients using diagnostic images of all coronary arteries,

Table 5 Coronary anomalies diagnosed based on surgical findings and/or conventional cardiac angiography

	n
Single coronary artery	3
LCX originating from RCC	2
LAD originating from RCC	1
RCA originating from LCC	1
Coronary-RV fistula	1

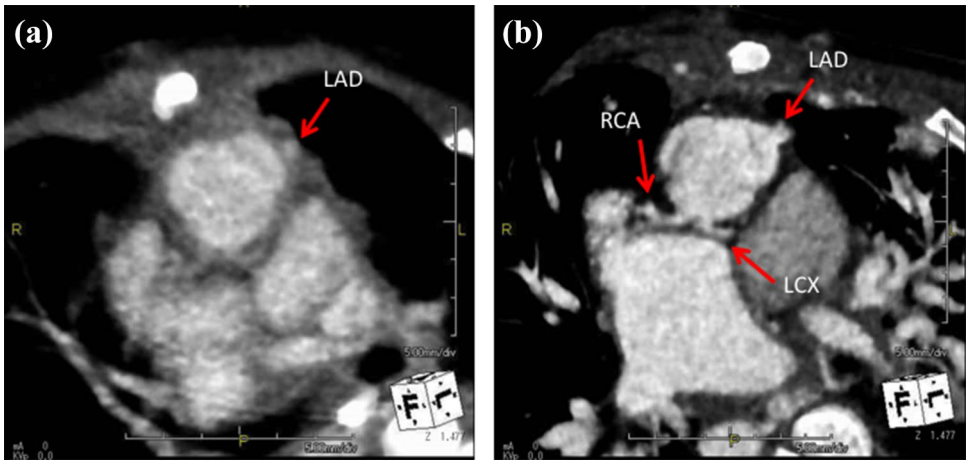

Fig. 2 A boy with a diagnosis of congenitally corrected transposition of the great arteries at the age of 1 month (**a**) and 1 year and 6 months (**b**). **a** Thick-section oblique-axial image showing the left anterior descending artery. The coronary score is 2 points (BW 2.60 kg, Ao CT value 245 H.U.). **b** Thick-section oblique-axial image showing all coronary arteries clearly: the right coronary artery and left circumflex artery are arising from the same cusp. The coronary score is 4 points (BW 8.11 kg, Ao CT value 332 H.U.). *RCA* right coronary artery, *LAD* left anterior descending artery, *LCX* left circumflex artery

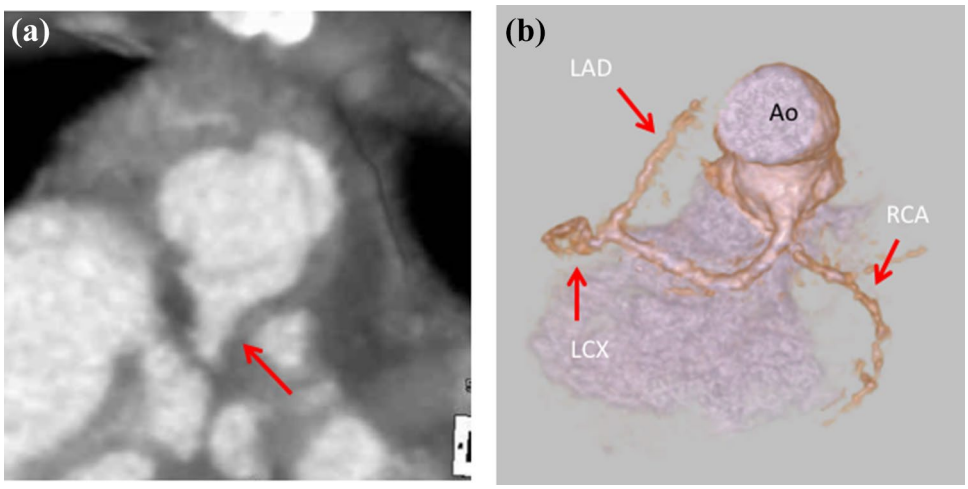

Fig. 3 A 9-month-old boy with a diagnosis of complete atrioventricular septal defect and a hypoplastic left ventricle. The coronary score is 4 points (BW 7.3 kg, Ao CT value 376 H.U.). **a** Thick-section oblique-axial image showing a single coronary artery arising from a left coronary cusp. **b** Volume rendered image of the single coronary artery. *RCA* right coronary artery, *LAD* left anterior descending artery, *LCX* left circumflex artery

ECG-triggered volume target scanning and hybrid iterative reconstruction allows high visibility of the coronary arteries in infants with complex CHD. Further, multivariate regression analysis showed significant correlations between the coronary score and body weight and between the coronary score and the CT value in the ascending aorta.

CCA is a recognized gold standard method for evaluating the coronary arteries, but catheterization of an infant, especially one with complex CHD, may be rather difficult because of the patient's size and inability to cooperate. Moreover, CCA is an invasive procedure with an approximately 1% intraoperative mortality [11], and there is the potential for high radiation doses [12]. Evaluation of the coronary ostium and the vessels using low-dose, non-invasive CTA may be useful in the clinic and for decision-making before surgery.

In infants, body size is an important determinant of the visibility of organ structures, including the coronary arteries. In general, the larger the organ structures become, the more clearly it can be seen. The results of our study can be considered acceptable in this regard. More recently, ultra-high-resolution CT has started to enter clinical use and would be useful for depicting the coronary arteries in infants [13].

In adults, coronary attenuation affects assessment of the coronary arteries, and optimization of coronary attenuation is crucial [14–16]. Our findings are consistent with previous reports in adults, demonstrating that coronary attenuation is important even in infants. In our study, we acquired CT images with slow infusion of contrast material. The venous

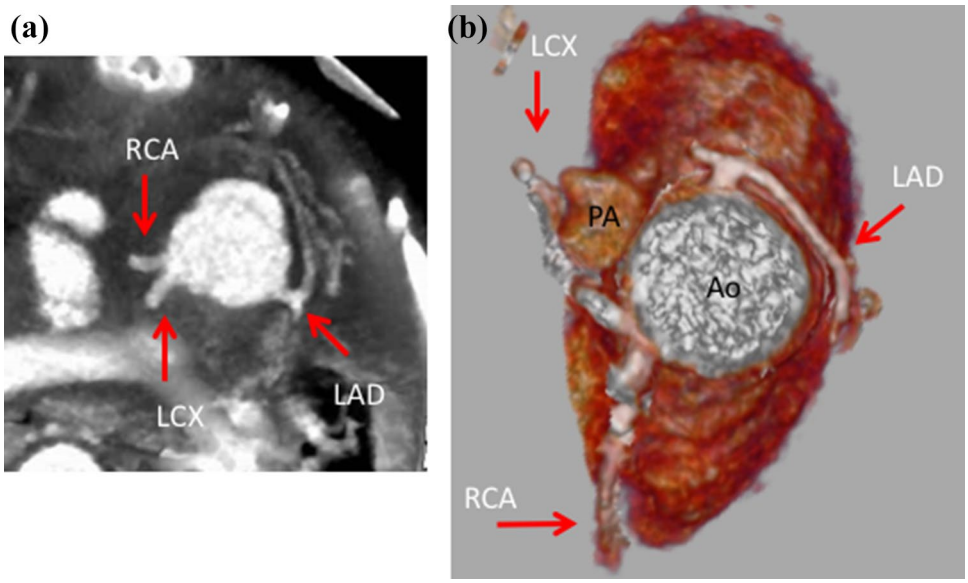

Fig. 4 A 19-month-old boy with a diagnosis of a single right ventricle. The coronary score is 4 points (BW 11.1 kg, Ao CT value 313 H.U.). **a** Thick-section oblique-axial image showing the right coronary artery and left circumflex artery arising from the same cusp. **b** Volume rendered image of the anomalous origin of left circumflex artery. *RCA* right coronary artery, *LAD* left anterior descending artery, *LCX* left circumflex artery

systems are more important structures in children than in adults because venous malformations are more common in children and preoperative evaluation for Glenn and Fontan procedures needs information on the venous system. Our scan protocol targeted both the arterial and venous structures, so there was no requirement for bolus injection or scans with earlier timing. Further studies of coronary attenuation in paediatric cardiac CT would be required.

However, the radiation exposure dose and image noise were not related to the visibility of the coronary arteries. In this study, image noise was controlled at a low level (noise level: standard deviation = 20, thickness = 0.5 mm) using automatic exposure control to maintain image quality for clinical use. These parameters would not affect the visibility of coronary arteries in the range of possible clinical situations outlined here.

To avoid unnecessary irradiation, it is important for radiologists to know the limitations of using CT to detect coronary arteries. This knowledge, in addition to understanding the factors that can influence image quality, should be of value in the clinical setting.

This study has several limitations. First, the study population was rather small. Second, we combined prospective ECG-triggered volume target scanning, a tube voltage with a setting of 80 kV, and hybrid iterative reconstruction to reduce the radiation dose without impairing image quality. However, the radiation exposure in our study was somewhat higher than that reported previously [4, 17, 18] and might have been caused by wide craniocaudal-directional coverage. Patients with complex CHD are also likely to have extracardiac malformations, such as an anomalous trachea, which had a high prevalence in our study. Assessment of the bronchial tree, thymus, and isomerism is important in the clinical management of complex CHD. In addition, the tube current was set by automatic exposure control and image noise was controlled at a low level to maintain image quality for clinical use, as previously mentioned. This could also have been the source of the excessive irradiation.

In conclusion, second-generation 320-row CTA with prospective ECG-triggered volume target scanning and hybrid iterative reconstruction allows good visibility of the coronary arteries in infants with complex CHD. Body weight and the CT value in the ascending aorta are important factors influencing the visibility of coronary arteries in this age group. The patients with body weight > 4.74 kg might be suitable candidates for coronary artery assessment with 320-row CTA.

Acknowledgement This work was supported by the Japan Society for the Promotion of Science (JSPS) KAKENHI (17K16452).

Compliance with ethical standards

Conflict of interest Satoshi Kawanami: Bayer Healthcare Japan, Modest, Research Grant; Philips Electronics Japan, Modest, Research Grant. Other authors: none.

References

1. Ruzmetov M, Jimenez MA, Pruitt A, Turrentine MW, Brown JW (2005) Repair of tetralogy of Fallot with anomalous coronary arteries coursing across the obstructed right ventricular outflow tract. Pediatr Cardiol 26:537–542
2. Goo HW, Seo DM, Yun TJ et al (2009) Coronary artery anomalies and clinically important anatomy in patients with congenital heart disease: multislice CT findings. Pediatr Radiol 39:265–273
3. Massoudy P, Baltalarli A, de Leval MR et al (2002) Anatomic variability in coronary arterial distribution with regard to the arterial switch procedure. Circulation 106:1980–1984

4. Zhang T, Wang W, Luo Z et al (2012) Initial experience on the application of 320-row CT angiography with low-dose prospective ECG-triggered in children with congenital heart disease. Int J Cardiovasc Imaging 28:1787–1797
5. Nie P, Li H, Duan Y et al (2014) Impact of sinogram affirmed iterative reconstruction (SAFIRE) algorithm on image quality with 70 kVp-tube-voltage dual-source CT angiography in children with congenital heart disease. PLoS ONE 9:e91123
6. Sun Z, Choo GH, Ng KH (2012) Coronary CT angiography: current status and continuing challenges. Br J Radiol 85:495–510
7. Soongswang J, Nana A, Laohaprasitiporn D et al (2000) Limitation of transthoracic echocardiography in the diagnosis of congenital heart diseases. J Med Assoc Thai 83(Suppl 2):S111–S117
8. Shrimpton PC (2004) Assessment of patient dose in CT. NRPBPE/1/2004
9. Goo HW, Yang DH (2010) Coronary artery visibility in free-breathing young children with congenital heart disease on cardiac 64-slice CT: dual-source ECG-triggered sequential scan vs. single-source non-ECG-synchronized spiral scan. Pediatr Radiol 40:1670–1680
10. Goo HW, Park IS, Ko JK et al (2005) Visibility of the origin and proximal course of coronary arteries on non-ECG-gated heart CT in patients with congenital heart disease. Pediatr Radiol 35:792–798
11. Vitiello R, McCrindle BW, Nykanen D, Freedom RM, Benson LN (1998) Complications associated with pediatric cardiac catheterization. J Am Coll Cardiol 32:1433–1440
12. Bacher K, Bogaert E, Lapere R, De Wolf D, Thierens H (2005) Patient-specific dose and radiation risk estimation in pediatric cardiac catheterization. Circulation 111:83–89
13. Kakinuma R, Moriyama N, Muramatsu Y et al (2015) Ultra-high-resolution computed tomography of the lung: image quality of a prototype scanner. PLoS ONE 10:e0137165
14. Kawaguchi N, Kurata A, Kido T et al (2014) Optimization of coronary attenuation in coronary computed tomography angiography using diluted contrast material. Circ J 78:662–670
15. Cademartiri F, Maffei E, Palumbo AA et al (2008) Influence of intra-coronary enhancement on diagnostic accuracy with 64-slice CT coronary angiography. Eur Radiol 18:576–583
16. Fei X, Du X, Yang Q et al (2008) 64-MDCT coronary angiography: phantom study of effects of vascular attenuation on detection of coronary stenosis. AJR Am J Roentgenol 191:43–49
17. Cheng Z, Wang X, Duan Y et al (2010) Low-dose prospective ECG-triggering dual-source CT angiography in infants and children with complex congenital heart disease: first experience. Eur Radiol 20:2503–2511
18. Huang MP, Liang CH, Zhao ZJ et al (2011) Evaluation of image quality and radiation dose at prospective ECG-triggered axial 256-slice multi-detector CT in infants with congenital heart disease. Pediatr Radiol 41:858–866